

Figure S6. View of the $[N(CH_3)_4][OsO_4F]$ unit cell showing the packing along the b -axis.

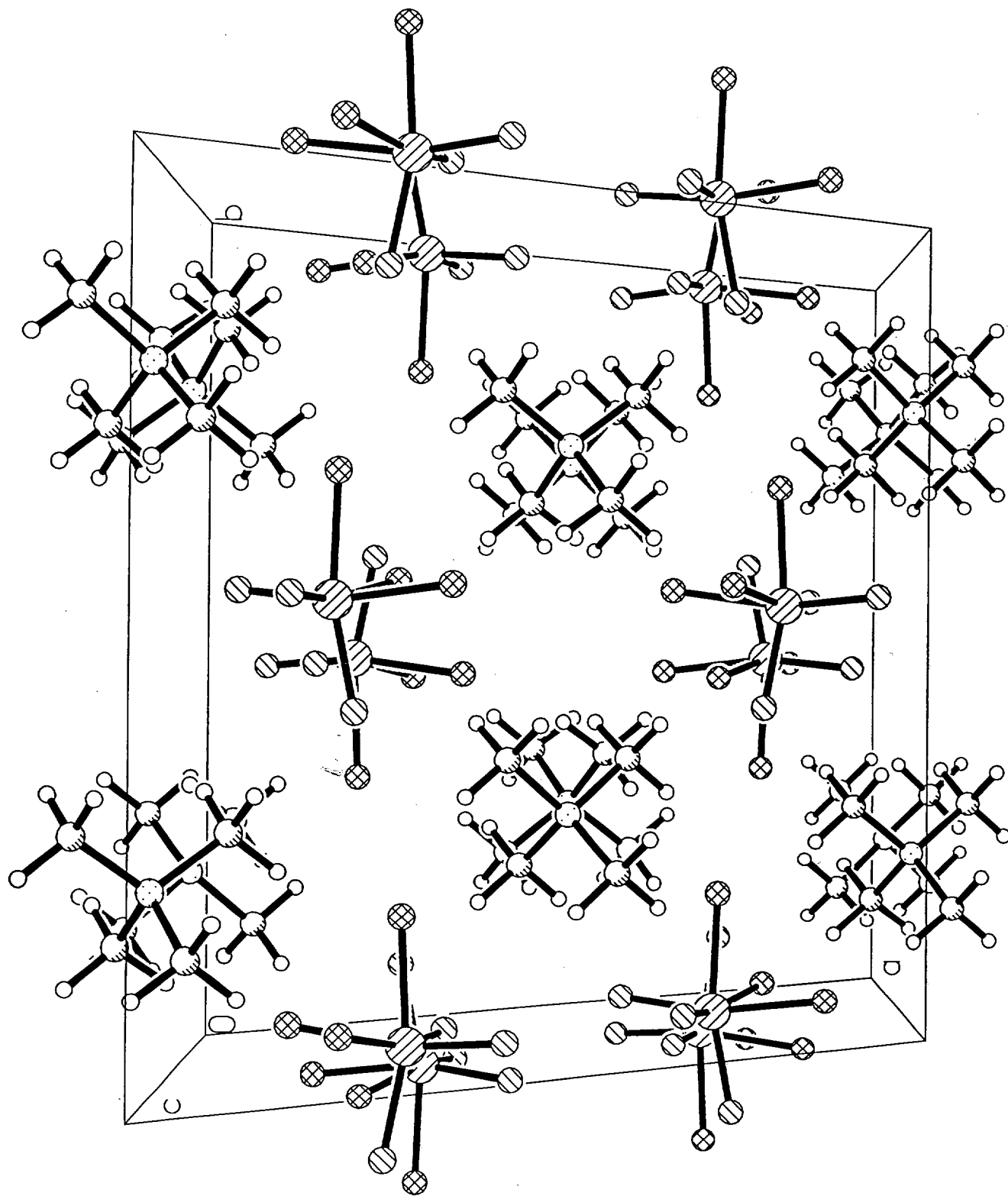


Figure S7. View of the $[N(CH_3)_4][OsO_3F_3]$ unit cell showing the packing along the c -axis.

Table S8. Correlation Diagram for the Vibrational Modes of the a) $\text{N}(\text{CH}_3)_4^+$ Cation and b) OsO_4F^- Anion in $[\text{N}(\text{CH}_3)_4][\text{OsO}_4\text{F}]$.^a

	Cation Symmetry, T_d	Site Symmetry, C_2	Crystal Symmetry, C_{2v}	
$4(\nu_1 - \nu_3)$	A_1	A	A_1 (Ra, IR)	$2(\nu_1 - \nu_8), 2(\nu_9 - \nu_{19}), 2R, 2T$
$4\nu_4$	A_2		A_2 (Ra)	$2(\nu_1 - \nu_8), 2(\nu_9 - \nu_{19}), 2R, 2\tilde{T}$
$4(\nu_5 - \nu_8)$	E			
$4(\nu_9 - \nu_{12}), 4R$	T_1		B_1 (Ra, IR)	$4(\nu_9 - \nu_{19}), 4R, 4T$
$4(\nu_{13} - \nu_{19}), 4T$	T_2		B_2 (Ra, IR)	$4(\nu_9 - \nu_{19}), 4R, 4T$
		B		
	Anion Symmetry, C_s	Site Symmetry, C_s	Crystal Symmetry, C_{2v}	
$4(\nu_1 - \nu_8), 8T, 4R$	A'	A'	A_1 (Ra, IR)	$2(\nu_1 - \nu_8), 4T, 2R$
			A_2 (Ra, IR)	$2(\nu_9 - \nu_{12}), 2T, 4R$
$4(\nu_9 - \nu_{12}), 4T, 8R$	A''	A''	B_1 (Ra)	$2(\nu_1 - \nu_8), 4T, 2R$
			B_2 (Ra)	$2(\nu_9 - \nu_{12}), 2T, 4R$

^a Correlation of the free anion symmetry of OsO_4F^- (C_s) to the anion site symmetry (C_s) and the unit cell symmetry (C_{2v}) (space group $Abm2$) predicts that the A' modes of the free anion are each split into A_1 and B_1 components in the Raman and infrared spectra. The A'' modes are expected to split into A_2 and B_2 components in the Raman spectrum while the splitting is not observed in the infrared spectrum. Correlation of the free cation symmetry of $\text{N}(\text{CH}_3)_4^+$ (T_d) to the cation site symmetry (C_2) and the unit cell symmetry (C_{2v}) predicts that all bands ($\nu_1 - \nu_{19}$) are Raman and infrared active. In the Raman spectrum, the bands $\nu_1 - \nu_8$ and $\nu_9 - \nu_{19}$ are expected to be factor-group split into A_1 and A_2 and into A_1, A_2, B_1 , and B_2 components, respectively. In the infrared spectrum, the bands $\nu_1 - \nu_8$ are not expected to be split while the bands $\nu_9 - \nu_{19}$ are expected to split into A_1, B_1 , and B_2 components.

Table S9. Correlation Diagram for the Vibrational Modes of the a) $\text{N}(\text{CH}_3)_4^+$ Cation and b) OsO_3F_3^- Anion in $[\text{N}(\text{CH}_3)_4][\text{OsO}_3\text{F}_3]$.^a

	Cation Symmetry, T_d	Site Symmetry, C_2	Crystal Symmetry, C_{2h}	
$4(\nu_1 - \nu_3)$	A_1	A	A_g (Ra)	$2(\nu_1 - \nu_8), 2(\nu_9 - \nu_{19}), 2R, 2T$
$4\nu_4$	A_2		B_g (Ra)	$4(\nu_9 - \nu_{19}), 4R, 4T$
$4(\nu_5 - \nu_8)$	E		A_u (IR)	$2(\nu_1 - \nu_8), 2(\nu_9 - \nu_{19}), 2R, 2T$
$4(\nu_9 - \nu_{12}), 4R$	T_1		B_u (IR)	$4(\nu_9 - \nu_{19}), 4R, 4T$
$4(\nu_{13} - \nu_{19}), 4T$	T_2			
		B		
	Anion Symmetry, C_{3v}	Site Symmetry, C_1	Crystal Symmetry, C_{2h}	
$8(\nu_1 - \nu_4), 8T$	A_1	A	A_g (Ra)	$2(\nu_1 - \nu_5), 4(\nu_6 - \nu_{11}), 6T, 6R$
			B_g (Ra)	$2(\nu_1 - \nu_5), 4(\nu_6 - \nu_{11}), 6T, 6R$
$8\nu_5, 8R$	A_2		A_u (IR)	$2(\nu_1 - \nu_5), 4(\nu_6 - \nu_{11}), 6T, 6R$
			B_u (IR)	$2(\nu_1 - \nu_5), 4(\nu_6 - \nu_{11}), 6T, 6R$
$8(\nu_6 - \nu_{11}), 8R, 8T$	E			

^a Correlation of the free anion symmetry of OsO_3F_3^- (C_{3v}) to the anion site symmetry (C_1) and the unit cell symmetry (C_{2h}) (space group $C2/c$) predicts that all the vibrational bands are Raman and infrared active and are split into A_g and B_g components and into A_u and B_u components in the Raman and infrared spectrum, respectively. Correlation of the free cation symmetry of $\text{N}(\text{CH}_3)_4^+$ (T_d) to the cation site symmetry (C_2) and the unit cell symmetry (C_{2h}) predicts that all bands are Raman and infrared active. In the Raman and infrared spectra $\nu_1 - \nu_8$ are not expected to show factor-group splitting, while $\nu_9 - \nu_{19}$ are expected to be factor-group split into A_g and B_g components and into A_u and B_u components in the Raman and infrared spectrum, respectively.